Phase transformation yield surface determination for some shape memory alloys

Christian Lexcellent, Pascal Blanc

Phase transformation yield surface determination for some shape memory alloys

C. Lexcellent *, P. Blanc

Laboratoire de Mécanique Appliquée R. Chaléat, UMR 6604, CNRS-Université de Franche-Comté, 24 rue de l'Epitaphe, 25000 Besançon, France

Like in the "plasticity" theory, the prediction of phase transformation yield surfaces constitutes an essential issue in the mod-elling of polycrystalline shape memory alloys thermomechanical behaviour. Usually for "micro–macro" integration, the nature of the interface between austenite and twinned or untwinned martensite under stress free state and the choice of correspondence variants (CV) or habit plane variant (HPV) are predominant toward the explicit shape of the phase transformation surface. If the predictions for Cu–Al–Be, Cu–Al–Zn (interface between austenite and one single variant of martensite for cubic to monoclinic phase transformation) and Cu–Al–Ni (interface between austenite and twinned martensite for cubic to orthorhombic phase transformation) are fairly good; the prediction is not efficient in the important case of Ti–Ni (interface between austenite and twinned martensite with stress free state for cubic to monoclinic phase transformation). The usual hypothesis consisting in neglecting the effect of stress on the interface geometrical configuration ~must be revised.

Keywords: Microstructure; Interface; Phase transformation; Shape memory alloy

1. Introduction

Shape memory alloys (SMA) are materials undergoing a first order structural phase transformation. This phase transformation may be induced by a change either in stress or in temperature or both. These structural transformations occur in different ways from a high symmetry parent phase (called austenite) to a lower symmetry product phase (called martensite).

The deformation behaviour of SMA is predicted thanks to the knowledge of the different microstructures appearing during the transition between phases. As shown in [1], it is important to know such microstructures in order to predict the SMA thermomechanical response under various loading conditions.

At first, a theoretical analysis of the austenite–martensite transformation called WLR classical theory [2] was presented. It predicts the habit plane, orientation relationships and macroscopic distortions only from the knowledge of the crystal structures and lattice parameters of the parent and the product phases. Hence a martensite variant is identified by its own shape strain and habit plane normal vectors.

More recently, the theory used to construct microstructures is a geometrically non-linear theory of martensitic transformation performed by Ball and James [3,4]. These authors formulate a free energy function that would produce the A–M interface by energy minimization and relate it to crystal structure. One of the main results of this new theory (called crystallographic theory of martensite: CTM) is the recognition that some of the common microstructures in shape memory materials are possible (as energy minimizing microstructures) only with exceedingly special lattice parameters.

Generally speaking according to Bhattacharya [5], a single variant of martensite cannot have a coherent interface with the austenite. However a region consisting of fine twins of two martensitic variants can form a coherent interface with the austenite. But Hane [6] considered that alloys such as Cu–Al–Ni (cubic → monoclinic

* Corresponding author. Tel.: +33-381-666-052; fax: +33-381-666-700.

E-mail address: christian.lexcellent@univ-fcomte.fr (C. Lexcellent).

transformation) Cu–Zn, Cu–Zn–Al, Cu–Zn–Ga, etc. among others [7] exhibit an undeformed interface between austenite and a single variant of martensite.

For many alloys such as Ni–Ti, Cu–Al–Ni (cubic → orthorhombic transformation), the transformed region consists of parallel bands containing alternately two different variants of martensite. The CTM gives mathematical tools to predict untwinned or twinned martensite at the interface with the austenite phase.

However the different possible configurations at the interface A–M are predicted for the stress free state. For example, Shield [8] examines the effect of the crystalline orientation on the simple tension pseudoelastic behaviour of three different Cu–Al–Ni single crystals: "we will not consider elastic strains in the analysis presented here and will instead be using the "constrained theory" as described by Ball et al. [9]. Consistent with the way it was actually introduced, is that the elastic strains are neglected in comparison with the transformations strains.

In this context, considering the very recent paper [10] of Stupkiewicz and Petryk, who performed a new modelling of single crystal tensile tests of Shield [8]: "as a first approximation, in our model, we assume that the parameters describing the microstructure follow the two theories of martensite transformation [1,2], originally developed for the stress-free transformation".

As a summary, even for analysing the mechanical behaviour of SMA, the crystallographical microstructure is viewed as stress free. It means that exact compatibility of the transformation strains at zero stress is adopted.

The main question of the present paper consists in the workability of this important hypothesis. In this aim, a comparison between theoretical predictions of the initiation surface of phase transformation and experimental points for biaxial proportional loadings (tension (compression)–torsion, bicompression tests) is done.

Two microstructural configurations are investigated, (i) the coherent interface between austenite and one single variant of martensite (cubic → monoclinic) exhibited by Cu–Al–Be and Cu–Al–Zn for special compositions, (ii) the transformed region consists of parallel bands including alternately two different variants of martensite exhibited for instance by Ni–Ti (cubic → monoclinic) and Cu–Al–Ni (cubic → orthorhombic).

2. Austenite–martensite possible interfaces

2.1. General considerations

Let the reference configuration be unloaded and undistorded austenite at a temperature above the phase transformation temperature (A → M) in the three dimensional space. Considering any other configuration of the crystal as a deformation $\vec{y}(\vec{x})$. We assume that $\vec{y}(\vec{x})$ is continuous and piecewise continuously differentiable.

Therefore $\underline{F} = \nabla\vec{y}(\vec{x})$ is a piecewise continuous function. Moreover, if $\underline{F}$ is discontinuous across some surface, the jump in $\underline{F}$ across the surface must be a rank-one matrix. This is the Hadamard jump condition or compatibility condition (see [5] and the references therein). It ensures that the interface is coherent.

If $\vec{n}$ is unit vector normal to the interface, it means that for some vector $\vec{a}$, the matrices $\underline{F}_1$ and $\underline{F}_2$ representing the deformation gradient on each side of the interface must comply with

$$\underline{F}_2 - \underline{F}_1 = \vec{a} \otimes \vec{n}. \tag{1}$$

The polar decomposition theorem allows to decompose $\underline{F}$ (with positive determinant) uniquely as a product $\underline{Q}\underline{U}$ of a positive definite symmetric matrix $\underline{U} = (\sqrt{\underline{F}^{\mathrm{T}}\underline{F}})$ and a rotation $\underline{Q}$.

Let the homogeneous deformation $\vec{y} = \underline{U}_i\vec{x}$ take the austenite to the martensite. The matrix $\underline{U}_i$ is known as the Bain strain or the transformation stretches matrix.

Considering the distinct matrix of the form $\underline{R}^{\mathrm{T}}\underline{U}_i\underline{R}$ ($\underline{R}$: rotation matrix belonging to the point group of austenite) $\underline{U}_1, \underline{U}_2, \ldots, \underline{U}_v$. The integer v is given by [5]

$$v = \frac{\text{order of } P_{\mathrm{a}},\ \text{the point group of the austensite}}{\text{order of } P_{\mathrm{m}},\ \text{the point group of the martensite}}, \tag{2}$$

v represents the number of martensite variants.

It depends on the nature of the crystallographic transformation ($v = 3$ for cubic → tetragonal, $v = 6$ for cubic → orthorhombic, $v = 12$ for cubic → monoclinic, etc.).

2.2. Cubic to monoclinic phase transformations

Some copper based and Ni–Ti alloys exhibit a phase transformation between a cubic parent phase A (lattice parameter a_0) and a product phase M which is monoclinic (lattice parameters a, b, c and θ angle between the edges with lengths a and c).

The strain gradient tensor $\underline{F}$ can be written as

$$\underline{F} = \begin{pmatrix} \alpha & \gamma\cos\theta & 0 \\ 0 & \gamma\sin\theta & 0 \\ 0 & 0 & \beta \end{pmatrix}_{(\text{frame of A})}, \tag{3}$$

where the transformation stretches are

$$\alpha = \frac{\sqrt{2a}}{a_0}, \quad \beta = \frac{b}{a_0} \quad \text{and}$$

$$\gamma = \frac{\sqrt{2c}}{9a_0}\ (\text{M18R})\ [11,12] \quad \text{or} \quad \gamma = \frac{\sqrt{2c}}{3a_0}\ (6\text{M})\ [13]$$

$$\text{or} \quad \alpha = \frac{a}{a_0}, \quad \beta = \frac{b}{\sqrt{2}a_0} \quad \text{and}$$

$$\gamma = \frac{c}{\sqrt{2}a_0} \quad \text{for Ni–Ti[1].}$$

Hence, $\underline{U}^2 = \underline{F}^{\mathrm{T}}\underline{F}$ can be obtained

$$\underline{U}^2 = \begin{pmatrix} \alpha^2 & \alpha\gamma\cos\theta & 0 \\ \alpha\gamma\cos\theta & \gamma^2 & 0 \\ 0 & 0 & \beta^2 \end{pmatrix}_{(\text{frame of A})}, \quad (4)$$

In addition, the eigenvalues λ_1, λ_2 and λ_3 of this symmetric matrix are

$$\lambda_1 = \beta^2,$$
$$\lambda_2 = \frac{\alpha^2+\gamma^2-\sqrt{(\alpha^2-\gamma^2)^2+4\alpha^2\gamma^2\cos^2\theta}}{2}, \quad (5)$$
$$\lambda_3 = \frac{\alpha^2+\gamma^2+\sqrt{(\alpha^2-\gamma^2)^2+4\alpha^2\gamma^2\cos^2\theta}}{2}.$$

With the usual values of α, β, γ, obtained with lattice parameters X-ray measurements for these alloys, one obtains

$$\lambda_1 \leqslant \lambda_2 \leqslant \lambda_3. \quad (6)$$

Following Ball and James [3,4] an interface exists between austenite and a single variant of martensite called M_i $(i = 1, \ldots, 12)$ if and only if the symmetric matrix $\underline{U}^2$ has a first eigenvalue less than or equal to one (called λ_1), a second one equal to one (λ_2). And the third eigenvalue is greater than or equal to one (called λ_3).

$\underline{U}^2$ has an eigenvalue $\lambda_2 = 1$ if and only if, the monoclinic angle and the transformation stretches α and γ are related by

$$\cos^2\theta = \frac{(1-\alpha^2)(1-\gamma^2)}{\alpha^2\gamma^2}. \quad (7)$$

For instance, this situation is fulfilled for some copper based alloys [6,14] but not for Ni–Ti alloys (Eq. (7) and λ_i values) (see Table 1) as it has been verified.

It should be pointed out that the same calculations are made on the alloys Cu–23.73 Zn–9.4 Al and Cu–24.2 Al–2.95 Be than on the other copper based alloys [14], but with the measured lattice parameters we find λ_2 respectively equal to 0.98 and 0.979.

However with the first alloy, it was observed "in situ" (optical observation: $G = 50$) interfaces between austenite and single variant martensite by Lexcellent et al. [14].

For the second alloy, the sample observed has not exactly the same composition than Cu–24.2 Al–2.95 Be [12], that is why the results may be not completely exact. Nevertheless some copper based alloys were observed and give the same result. Following the theoretical analysis of James and Hane [15] λ_2 must be equal to one in order to insure the existence of an interface between austenite and a single variant of martensite.

2.2.1. Austenite – single variant of martensite microstructure

The previous discussion means that the "habit plane equation" and the monoclinic variant $\underline{U}_i$ $(i = 1, \ldots, 12)$

$$\underline{R}_i\underline{U}_i - \underline{1} = \vec{b} \otimes \vec{m} \quad (8)$$

give values for $\underline{R}_i$ (rotation matrix), $\vec{m}$: habit plane normal and $\vec{b}$: the shape strain vector.

Besides, with the eigenvalues from Eq. (5), it can be shown that the shape strain vector $\vec{b}$ and the habit plane normal $\vec{m}$ have components such as

$$\vec{b} = \frac{\sqrt{\alpha^2+\gamma^2-1}-\beta}{\sqrt{2}\sqrt{\alpha^2+\gamma^2-1-\beta^2}} \times \begin{pmatrix} \sqrt{2}\sqrt{\alpha^2+\gamma^2-1}\sqrt{1-\beta^2} \\ -\beta k\left(\sqrt{\gamma^2-1}+\sqrt{\alpha^2-1}\right) \\ \beta k\left(\sqrt{\gamma^2-1}-\sqrt{\alpha^2-1}\right) \end{pmatrix}_{(\text{austenite frame})}, \quad (9)$$

$$\vec{m} = \frac{1}{\sqrt{2}\sqrt{\alpha^2+\gamma^2-1-\beta^2}} \times \begin{pmatrix} -\sqrt{2}\sqrt{1-\beta^2} \\ -k\left(\sqrt{\gamma^2-1}+\sqrt{\alpha^2-1}\right) \\ k\left(\sqrt{\gamma^2-1}-\sqrt{\alpha^2-1}\right) \end{pmatrix}_{(\text{austenite frame})}, \quad (10)$$

where $k = \pm 1$. Thus, two solutions of the habit plane Eq. (8) exist.

At last, it can be found that the components of the symmetric matrix $\underline{U}$ in the austenite frame are

Table 1
Lattice parameters (Å) of cubic austenite and monoclinic martensite and obtained eigenvalues

Atomic composition	Austenite	Martensite				Eigenvalues		
	a_0	a	b	c	θ	γ_1	λ_2	λ_3
Cu–15 Zn–17 Al [6] ($L_{2_1} \rightarrow 6M$)	5.996	4.553	5.452	13.014	94.2	0.827	1.004	1.196
Cu–14 Al–4 Ni [6]($L_{2_1} \rightarrow 6M$)	5.836	4.430	5.330	12.79	95.6	0.834	0.994	1.226
Cu–20 Zn–12 Ga [6] ($L_{2_1} \rightarrow 6M$)	5.86	4.40	5.33	12.78	94.9	0.827	0.993	1.192
Cu–23.73 Zn–9.4 Al [11]	5.870	4.441	5.330	38.132	89.08	0.824	0.980	1.218
Cu–24.2 Al–2.95 Be [12]	5.82	4.46	5.22	38.25	83.3	0.804	0.979	1.262
Ti–49.2 Ni [1]	3.015	2.898	4.108	4.646	97.78	0.862	0.928	1.249
Ti–49.75 Ni [1]	3.015	2.889	4.12	4.622	96.80	0.869	0.934	1.224

$$\underline{U} = \begin{pmatrix} \beta & 0 & 0 \\ 0 & \xi_1 + 2\xi_2 + \xi_3 & \xi_1 - \xi_3 \\ 0 & \xi_1 - \xi_3 & \xi_1 - 2\xi_2 + \xi_3 \end{pmatrix}, \tag{11}$$

where

$$\begin{cases} \xi_1 = \dfrac{\gamma^2 - 1 + (\alpha^2 - 1)\sqrt{\alpha^2 + \gamma^2 - 1}}{2(\alpha^2 + \gamma^2 - 2)}, \\ \xi_2 = \left(\sqrt{\alpha^2 + \gamma^2 - 1} - 1\right)\dfrac{\sqrt{(\alpha^2 - 1)(\gamma^2 - 1)}}{2(\alpha^2 + \gamma^2 - 2)}, \\ \xi_3 = \dfrac{\alpha^2 - 1 + (\gamma^2 - 1)\sqrt{\alpha^2 + \gamma^2 - 1}}{2(\alpha^2 + \gamma^2 - 2)}. \end{cases} \tag{11bis}$$

As recalled before, there are twelve distinct variants $\underline{U}_1, \ldots, \underline{U}_{12}$. For example, the components of the variant $\underline{U}_1$ can be taken as these given in Eq. (11).

While the remaining variants are found from this variant by a symmetry transformation using the rotation in the cubic Laüe Group $(\mathfrak{L}^c = \mathfrak{P}_a \cap S_0(3))$.

As a summary, there are 24 distinct possible couples $(\vec{b}_i, \vec{m}_i)$ in that kind of phase transformation.

2.2.2. Austenite–twinned martensite microstructure

The austenite–twinned martensite microstructure configuration is given in Fig. 1. It consists of two adjacent regions: in the first one the austenite phase is present, the other one contains parallel bands of alternating layers of two martensite variants. According to Ball and James [3,4] with the martensite variant pair (i, j) the compatibility equations are

(i) the twinning equation between the martensite variants i and j itself

$$\underline{R}_{ij}\underline{U}_i - \underline{U}_j = \vec{a} \otimes \vec{n}, \tag{12}$$

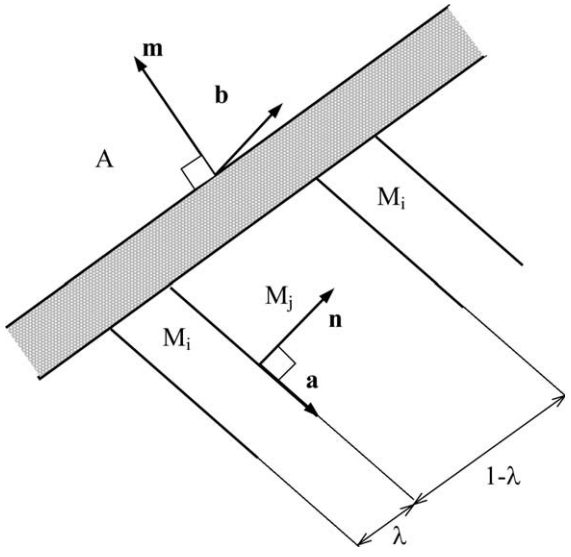

Fig. 1. Schematic view of a laminated austenite–twinned martensite microstructure (A: austenite, M_i, M_j: martensite variants).

(ii) the habit plane equation written

$$\overline{R}_{ij}(\lambda \underline{R}_{ij}\underline{U}_i + (1 - \lambda)\underline{U}_j) - 1 = \vec{b} \otimes \vec{m}. \tag{13}$$

The algorithm to find the solutions is given in the paper [1].

In a first step, the resolution of the twinning Eq. (12) delivers the pairs (i, j) which are compatible. They are often called the correspondence variants CV. For Ni–Ti, there are 132 correspondence variant pairs. Among these there are 84 (sets S_1, S_2, S_3, S_4) where the set (i, j) contains also the set (j, i). The last 48 (sets S_5 and S_6) of CV pairs are rather odd because they do not individually contains both variants pairs (i, j) and (j, i) but appears only for a special choice of the lattice parameters.

Secondly, the resolution of the habit plane equation permits to choose among the CV pairs, the so-called habit plane variant (HPV) which is a compound twin of $\lambda \underline{U}_i$ and $(1 - \lambda)\underline{U}_j$. At last for Ni–Ti 192 different couples of $(\vec{b}_{ik}, \vec{m}_{jk})$ are obtained (with $i, j = 1$–12, $i \neq j$, $k = 1$–8).

It should be noted that for both alloys: Ti–49.2 Ni (wt%) and Ti–49.75 Ni (wt%), we are in this case. Indeed for many couples (i, j), the matrix C_{ij} (Eq. (15)) has an eigenvalue equal to 1 for a suitable choice of λ.

If the twinning Eq. (12) is substituted in the habit plane Eq. (13), then the habit plane equation becomes

$$\overline{R}_{ij}(\underline{U}_j + \lambda \vec{a} \otimes \vec{n}) - 1 = \vec{b} \otimes \vec{m}. \tag{14}$$

Let the symmetric matrix $\underline{C}_{ij}(\lambda)$ defined by

$$C_{ij}(\lambda) = (\underline{U}_j + \lambda \vec{a} \otimes \vec{n})^{\mathrm{T}}(\underline{U}_j + \lambda \vec{a} \otimes \vec{n}). \tag{15}$$

If $\vec{e}_1$ and $\vec{e}_3$ are the eigenvectors corresponding to the eigenvalues λ_1 and λ_3 of $\underline{C}_{ij}(\lambda)$ $(\lambda_1 \leqslant \lambda_2 = 1 \leqslant \lambda_3)$, it can be demonstrated that

$$\vec{b} = \frac{\sqrt{\lambda_3} - \sqrt{\lambda_1}}{\sqrt{\lambda_3 - \lambda_1}}\left(\sqrt{\lambda_3(1 - \lambda_1)}\vec{e}_1 + k\sqrt{\lambda_1(\lambda_3 - 1)}\vec{e}_3\right)$$

and (16)

$$\vec{m} = \frac{1}{\sqrt{\lambda_3 - \lambda_1}}\left(-\sqrt{1 - \lambda_1}\vec{e}_1 + k\sqrt{\lambda_3 - 1}\vec{e}_3\right),$$

with $k = \pm 1$.

2.3. Cubic to orthorhombic transformation (examination of Cu–13.95 Al–3.93 Ni (wt%))

In a very simple way, $\underline{U}^2 = (\underline{F}^{\mathrm{T}}\underline{F})$ can be expressed as

$$\underline{U}^2 = \begin{pmatrix} \dfrac{\alpha^2 + \gamma^2}{2} & \dfrac{\alpha^2 - \gamma^2}{2} & 0 \\ \dfrac{\alpha^2 - \gamma^2}{2} & \dfrac{\alpha^2 + \gamma^2}{2} & 0 \\ 0 & 0 & \beta^2 \end{pmatrix}_{\text{(austenite frame)}}, \tag{17}$$

with $\alpha = 1.0619$, $\beta = 0.9178$ and $\gamma = 1.023$ (obtained for Cu–14.2 Al–4.3 Ni (wt%) [16,17]).

The eigenvalues are evidently: $\lambda_1 = \beta^2$, $\lambda_2 = \gamma^2$, $\lambda_3 = \alpha^2$ and $\lambda_2 = 1.046$ is different from 1. However,

according to our calculations (Eq. (15)) with the values above, we find a root $\lambda_2' = 1$. $\underline{C}_{ij}$ eigenvalues confirms the presence of an interface between austenite and twinned martensite.

Using procedure (2.2), we find that we can have an austenite–martensite interface with either twins I or II.

Interfaces using type I twin $\lambda = 0.2906$

$b^+ = (0.06565, 0.06573, 0.02379)$,

$b^- = (0.05763, -0.07473, 0.01700)$,

$\hat{m}^+ = (0.6355, -0.7484, 0.1897)$,

$\hat{m}^- = (0.7154, 0.6497, 0.2572)$.

Interfaces using type II twin $\lambda = 0.3011$

$b^+ = (0.05599, -0.07068, 0.02359)$,

$b^- = (0.06531, 0.06538, 0.01211)$,

$\hat{m}^+ = (0.7306, 0.6679, 0.1420)$,

$\hat{m}^- = (0.6350, -0.7275, 0.2599)$.

Thus, we have 96 A–M possible austenite–martensite interfaces in this material (48 type I, 48 type II) i.e. 96 different couples $(\vec{b}_i, \vec{m}_j)$.

Following Ichinose et al. [18], type I twins are 2.5 times harder to move than type II twins, thus during mechanical loadings, type II is expected to be observed.

It can be recalled that type I twins have one plane of symmetry while type II twins have none.

3. Phase transformation surface (austenite → martensite)

3.1. Theoretical considerations

Let have a biaxial "dead" loading i.e. the stress tensor will be expressed in the reference configuration,

$$\underline{\sigma} = \sigma_1 \vec{e}_1 \otimes \vec{e}_1 + \sigma_2 \vec{e}_2 \otimes \vec{e}_2. \tag{18}$$

The predicted phase transformation surface must be at least convex in the stress space (σ_1, σ_2) must also account for the general asymmetry between tension and compression observed in SMA and at last must fitted the experimental yield points obtained for proportional biaxial loadings in tension(compression)–torsion or bi-compression.

As a criterion the first variant appears when a thermodynamical force associated to the phase transformation is equal to zero:

$$\underline{\sigma} : \underline{\varepsilon}^{\mathrm{t}} - K(T) = 0, \tag{19}$$

where $\underline{\sigma}$ and $\underline{\varepsilon}^{\mathrm{t}}$ are naturally written in the geometrical frame of the sample. $\underline{\sigma} : \underline{\varepsilon}^{\mathrm{t}}$ represent the mechanical energy required to transform completely a unit volume of austenite into martensite. This hypothesis or assumption is for instance made by Patoor et al. [19] in some micro–macro modelling and also for some phenomenological investigation at the macro-scale [20] suggests.

If $\underline{R}$ is the rotation matrix from the austenite cell frame to the geometrical sample one, then

$$\underline{\varepsilon}^{\mathrm{t}} = {}^{\mathrm{T}}\underline{R}\underline{E}^{\mathrm{t}}\underline{R} \quad \text{with } \underline{E}^{\mathrm{t}} = \tfrac{1}{2}(\underline{U}^2 - \underline{1}), \tag{20}$$

$\underline{U} = \underline{U}_i$ $(i = 1, \ldots, v)$ for a single variant $\underline{U} = (1 - \lambda)\underline{U}_i + \lambda \underline{U}_j$ (with $(i, j) \in \{1, \ldots, v\}$) for a twinned variant.

The procedure used to calculate yield surface of polycrystal is purely phenomenological and is adapted from a paper by Huang [21]:

(i) A polycrystalline material is represented by n grains (here 1000 grains are chosen) defined by their crystallographic orientation. Obviously, an isotropic texture, which represents a random distribution of the grain crystallographic lattice orientation in the space of the Euler angles, is chosen. The number m of possible variants $\underline{U}_i$ is different for Ni–Ti or Cu–Al–Ni. Interactions between the grains are not taken into account. As the yield surface represents apparition of the first activated martensite platelets, interaction stresses are not playing an important part yet.

(ii) Under a given stress condition $\underline{\sigma}^0$, for each grain k and among the m possible variants, the one presenting the higher factor K (Eq. (12)) is selected. It should be noted that we use there a Sachs type model. Indeed, this variant is the one with the largest transformation strain along the stress direction, which is equivalent to the lowest transformation stress, it is similar to a Schmid law. A set of n factors $K_k^{\max}$ is determined by this method.

(iii) A new set of $K_k^{\max}$ can be calculated under a different stress condition. $K_{\mathrm{tension},k}^{\max}$ stands for the results under uniaxial tension.

(iv) The ratio called r and the phase transformation start stress $\underline{\sigma}^{\mathrm{t}}$ are obtained (Eq. (14)).

(v) A new stress condition is applied and the corresponding phase transformation stress is determined, and so on.

Hence, a convex yield surface in the biaxial stress space (σ_1, σ_2) is determined for the polycrystalline alloys.

$$r = \frac{\sum_{k=1,\ldots,n} K_k^{\max}}{\sum_{k=1,\ldots,n} K_{\mathrm{tension},k}^{\max}} \quad \text{and} \quad \underline{\sigma}^{\mathrm{t}} = \frac{1}{r}\underline{\sigma}^0. \tag{21}$$

3.2. Transformation surface prediction

There is also a prediction of these surfaces at the macroscopic scale. Like in the classical plasticity theory, a combination of the second (J_2) and the third (J_3) invariants of the deviatoric stress tensor dev $\underline{\sigma}$ is used [13,14,22].

This application constitutes the extension of a thermodynamical study of isotropic pseudoelasticity in

shape memory alloys considering the tension–compression assymmetry performed by Raniecki and Lexcellent [20]. Without entering into the details, the yield surface corresponds to the fact that the thermodynamical force associated to the volume fraction of martensite attains a zero value. As the volume variation associated to the phase transformation is negligible, only the two invariants of the stress deviator are taken into account.

Under isothermal conditions, the following yield surface is proposed

$$g(\sigma_{ij}) = \bar{\sigma} f(y) - \sigma_0 = 0, \tag{22}$$

with $\bar{\sigma}$ is the classical Von Mises invariant (second invariant of the deviatoric stress tensor)

$$\bar{\sigma} = \left(\frac{3}{2} \mathrm{dev}\,\underline{\sigma} : \mathrm{dev}\,\underline{\sigma} \right)^{1/2}, \tag{23}$$

J_3 is the third invariant of the deviatoric stress tensor

$$J_3 = \det(\mathrm{dev}\,\underline{\sigma}). \tag{24}$$

The adimensional parameter y is defined by

$$y = \frac{27}{2} \frac{J_3}{\bar{\sigma}^3}. \tag{25}$$

The choice of the $f(y)$ function corresponds to the necessity to have a convex yield surface for any chosen material parameter a.

For instance a choice of

$$f(y) = 1 + ay \tag{26}$$

is not convenient.

On the opposite, a more complicated equation of $f(y)$ like

$$f(y) = \cos\left(\frac{ar\cos(1 - a(1-y))}{3} \right) \quad \text{with} \quad -1 < a < 1 \tag{27}$$

works.

For the two copper-based alloys investigated (Cu–23.73 Zn–9.4 Al (at.%) and Cu–24.2 Al–2.95 Be (at.%) where an ''austenite–single variant martensite'' interface is predicted with stress free state, a good agreement is obtained between prediction and experiments (Figs. 2 and 3).

For the Cu–13.95 Al–3.93 Ni (wt%) which shows a cubic to orthorhombic transformation, it's considered that an interface between austenite and twinned martensite is predicted with stress free state. The micro–macro prediction (Fig. 4) seems consistent with the two previous shape yield curves obtained for the Cu–Zn–Al and Cu–Al–Be.

In particular, the established asymmetry in tension–compression for this alloys [10] is taken into account in the prediction.

The prediction for Ti – 49.75 Ni (at.%) with an austenite–twinned martensite interface with stress free state

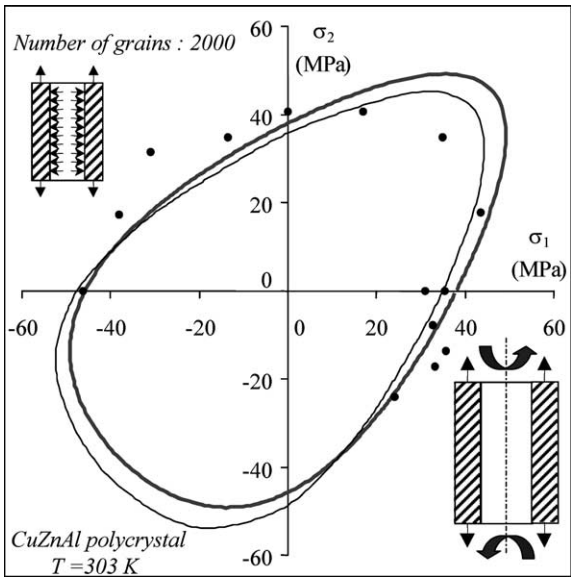

Fig. 2. Yield surface of Cu–Zn–Al polycrystal in the space (σ_1, σ_2) (austenite → untwinned martensite) (• experimental points; — micro–macro simulation; ─ phenomenological simulation).

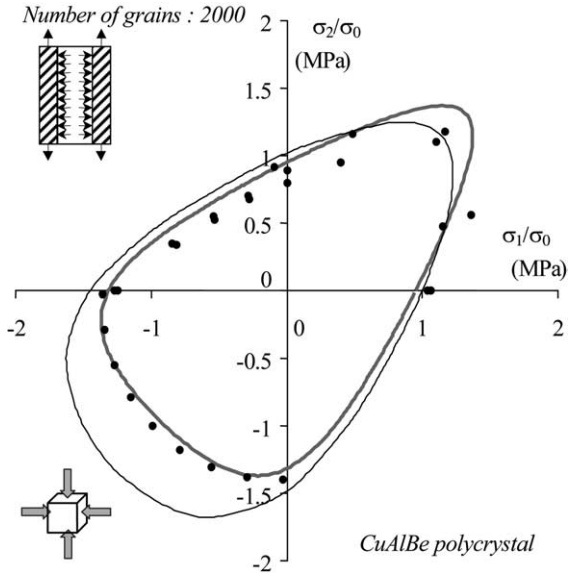

Fig. 3. Yield surface of Cu–Al–Be polycrystal in the space (σ_1, σ_2) (austenite → untwinned martensite) (• experimental points; — micro–macro simulation; ─ phenomenological simulation).

is more questionable (Fig. 5). For instance, the asymmetry between tension and compression which has been measured on this alloy [22,23] is not predicted.

This gap between prediction and real material behaviour for Ni–Ti is confirmed by the work of Patoor et al. [24]. In the very important case of this alloy, there is no agreement between the experimental results and the prediction. In order to solve the problem, they determined a new interaction matrix considering the existence of two CVs inside each HPV, without efficient results.

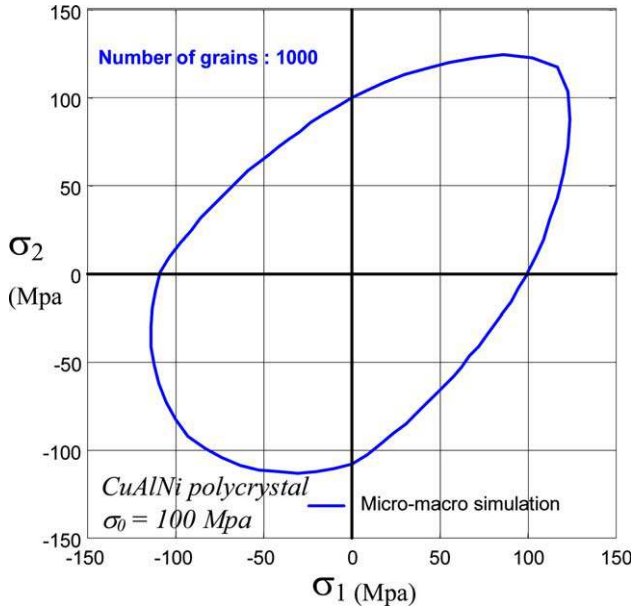

Fig. 4. Phase transformation surface of Cu–Al–Ni polycrystal in the space (σ_1, σ_2) (austenite → twinned martensite) (— micro–macro simulation).

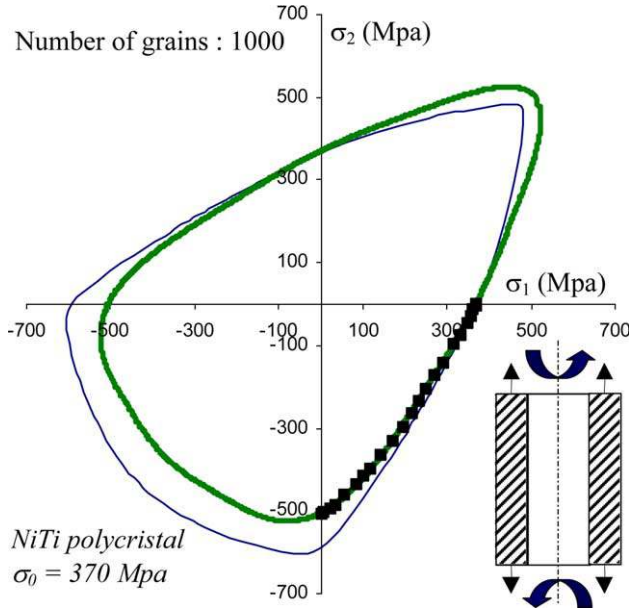

Fig. 6. Phase transformation surface of Ni–Ti polycrystal in the space (σ_1, σ_2) (austenite → martensite as if it was single martensite) (■ experimental points; — micro–macro simulation, ─ phenomenological simulation).

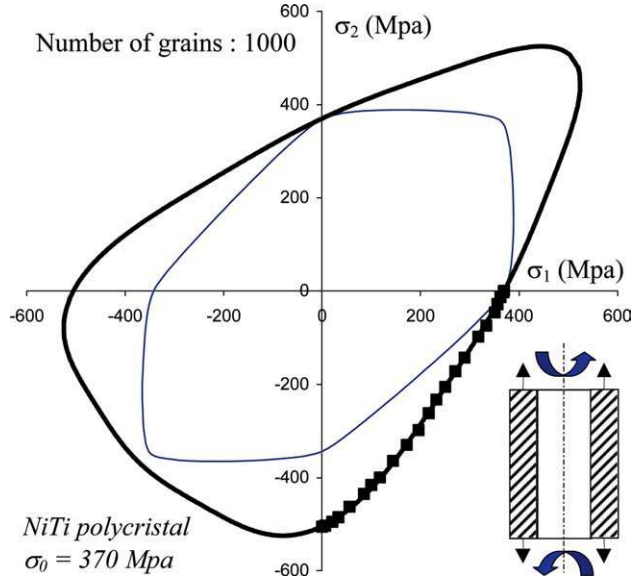

Fig. 5. Phase transformation surface of Ni–Ti polycrystal in the space (σ_1, σ_2) (austenite → twinned martensite) (■ experimental points; — micro–macro simulation, ─ phenomenological simulation).

Actually, the same investigation is done with the double Hadamard conditions whereas this interaction matrix and the obtained results are also not efficient. However for Cu–Zn–Al (case of the austenite → single variant martensite), the micro–macro approach [24] and our investigation give nearly the same yield phase transformation curve [14].

Our interpretation of this strange Ni–Ti behaviour is the following: it seems that the interface configuration (austenite–twinned martensite $\lambda \underline{U}_i + (1-\lambda)\underline{U}_j$) predicted with stress free state is not the same than under stresses. However, if one imagines that under stress for NiTi alloys, the variant which appears is untwinned, one can make the calculation with the single variant hypothesis and examines its prediction. The calculation seems to be in good agreement some experimental biaxial point and the macroscopic prediction (Fig. 6).

4. Conclusion

On the one hand, the crystallographic theory of martensite performed by Ball and James [3,4], Bhattacharya [5], Hane [6], Shield [8] permit to determine the nature of the interface i.e. between austenite and a single variant of martensite or between austenite and a twinned austenite, with stress free state.

The determination of the habit plane normal $\vec{m}$ and the shape strain vector $\vec{b}$ and the choice of a simple thermodynamical driving force permit to obtain the yield phase transformation criterion.

The yield surface prediction is efficient for some Cu–Zn–Al and Cu–Al–Be (austenite/untwinned martensite) and Cu–Al–Ni (austenite/twinned martensite) but not for Ni–Ti equiatomic alloys.

For these alloys, since the grains are very small (less than 1 μm size), the hypothesis of neglecting grain boundaries interaction can be revised as well as the

hypothesis of neglecting stress effect on the interface between austenite and martensite.

In spite of the observation difficulties, an "in situ" observation of Ni–Ti samples under loading, would interesting informations about this last point and real geography of the interface microstructure under stress certainly bring out.

Acknowledgements

The authors are very grateful to Professor John Ball (from Institute of Mathematics in Oxford) for fruitful discussions.

References

[1] Hane KF, Shield TW. Acta Mater 1999;47(9):2603.
[2] Wechsler MS, Lieberman DS, Read TA. Trans AIME 1953;197:1503.
[3] Ball JM, James RD. Arch Ration Mech Anal 1987;100:13.
[4] Ball JM, James RD. Phil Trans R Soc Lond A 1992;338:389.
[5] Bhattacharya K. Acta Metall Mater 1991;39(10):2431.
[6] Hane KF. J Mech Phys Solids 1999;47:1917.
[7] Funakubo H, editor. Shape memory alloys. New York: Gordon and Breach; 1987.
[8] Shield TW. J Mech Phys Solids 1995;43:869.
[9] Ball J, Chu C, James RD. J de Physique IV 1995;C8:245.
[10] Stupkiewicz S, Petryk H. J Mech Phys Solids 2002;50:2329.
[11] Satto C, Jansen J, Lexcellent C, Schryvers D. Solid State Commun 2000;116:273.
[12] Moreau F, Tidu A, Barbe A, Eberhadt A, Heizman JJ. J de Phys IV 1995;5(C2):269.
[13] Gillet Y, Patoor E, Berveiller M. J Int Mater Syst Struct 1998;9:366.
[14] Lexcellent C, Vivet A, Bouvet C, Calloch S, Blanc P. J Mech Phys Solids 2002;50:2717.
[15] James RD, Hane KF. Acta Mater 2000;48:197.
[16] Otsuka K, Shimizu K. Jpn J Appl Phys 1969;8:1196.
[17] Otsuka K, Shimizu K. Trans JIM 1974;15:103.
[18] Ichinose S, Funatsu Y, Otani N, Ichikawa T, Miyazaki S, Otsuka K. Proceedings of the International Symposium on Intermetallic compounds, Sendai, Japan, 1991. p. 263.
[19] Patoor E, Berveiller M. CISM courses and lecture: mechanics of solids with phase changes. Wien (NY): Springer; 1997. No 368.
[20] Raniecki B, Lexcellent C. Eur J Mech A/Solids 1998;17(2):185–205.
[21] Huang W. Acta Mater 1999;47(9):2769–76.
[22] Raniecki B, Tanaka K, Ziolkowski A. Mater Sci Res Int Special Tech Publication 2001;2:327.
[23] Orgeas L, Favier D. Acta Mater 1998;46(15):5579.
[24] Patoor E, Niclaeys C, Arbab Chirani S, Ben Zineb T. In: Sun QP, editor. IUTAM Symposium on Mechanics of Martensite Phase Transformation in Solids. New York: Kluwer Academic Publishers; 2002. p. 131.